Probing twist-2 GPDs through the exclusive photoproduction of a photon-meson pair at EIC and beyond

10th Workshop of the APS Topical Group on Hadronic Physics

Saad Nabeebaccus
IJCLab

April 14, 2023

Based on 2212.00655 and 2302.12026 with S. Wallon, L. Szymanowski, B. Pire, G. Duplančić, K. Passek-Kumerički

Introduction

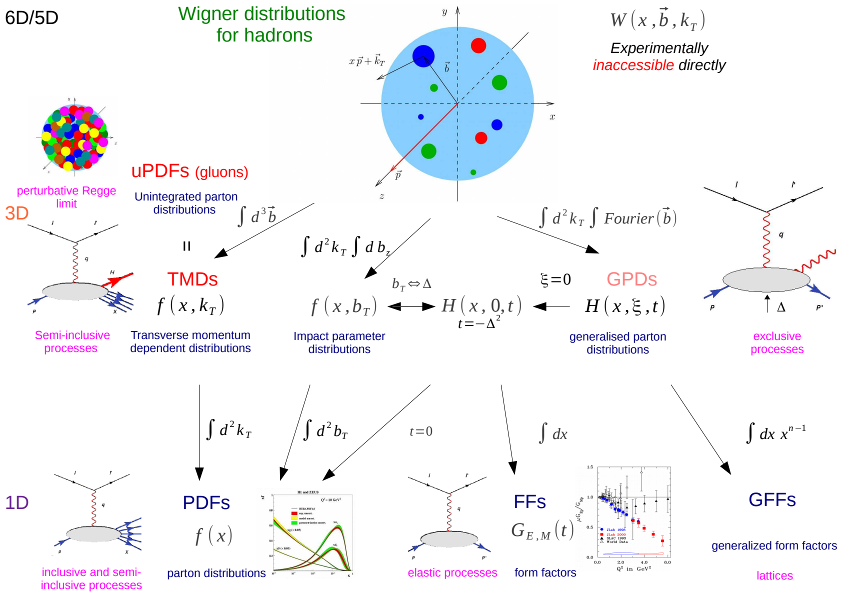

Quark GPDs at twist 2 [Diehl]

without helicity flip (chiral-even Γ matrices): 4 chiral-even GPDs:
(Note: $\Delta = p' - p$)

$$
\begin{aligned}
F^q &= \frac{1}{2}\int \frac{dz^-}{2\pi}\, e^{ixP^+z^-} \langle p'|\, \bar{q}(-\tfrac{1}{2}z)\, \gamma^+ q(\tfrac{1}{2}z)\, |p\rangle \Big|_{z^+=0,\, z_\perp=0} \\
&= \frac{1}{2P^+}\left[H^q(x,\xi,t)\, \bar{u}(p')\gamma^+ u(p) + E^q(x,\xi,t)\, \bar{u}(p')\frac{i\,\sigma^{+\alpha}\Delta_\alpha}{2m} u(p) \right],
\end{aligned}
$$

$$
\begin{aligned}
\tilde{F}^q &= \frac{1}{2}\int \frac{dz^-}{2\pi}\, e^{ixP^+z^-} \langle p'|\, \bar{q}(-\tfrac{1}{2}z)\, \gamma^+\gamma_5\, q(\tfrac{1}{2}z)\, |p\rangle \Big|_{z^+=0,\, z_\perp=0} \\
&= \frac{1}{2P^+}\left[\tilde{H}^q(x,\xi,t)\, \bar{u}(p')\gamma^+\gamma_5 u(p) + \tilde{E}^q(x,\xi,t)\, \bar{u}(p')\frac{\gamma_5\,\Delta^+}{2m} u(p) \right].
\end{aligned}
$$

$H^q \xrightarrow{\xi=0,t=0}$ PDF q $\qquad$ $\tilde{H}^q \xrightarrow{\xi=0,t=0}$ polarised PDF Δq

with helicity flip (chiral-odd Γ matrices): 4 chiral-odd GPDs:

$$\frac{1}{2}\int \frac{dz^-}{2\pi}\, e^{ixP^+z^-}\langle p'|\,\bar{q}(-\tfrac{1}{2}z)\, i\,\sigma^{+i}\, q(\tfrac{1}{2}z)\,|p\rangle\Big|_{z^+=0,\, z_\perp=0}$$

$$= \frac{1}{2P^+}\bar{u}(p')\left[H_T^q\, i\sigma^{+i} + \tilde{H}_T^q\,\frac{P^+\Delta^i - \Delta^+P^i}{m^2} + E_T^q\,\frac{\gamma^+\Delta^i - \Delta^+\gamma^i}{2m} + \tilde{E}_T^q\,\frac{\gamma^+P^i - P^+\gamma^i}{m}\right] u(p)\,,$$

$H_T^q \xrightarrow{\xi=0,t=0}$ quark transversity PDFs δq

Note: $\tilde{E}_T^q(x,-\xi,t) = -\tilde{E}_T^q(x,\xi,t)$

- Transverse spin content of the proton:

$$\begin{array}{ccc} |\uparrow\rangle_{(x)} & \sim & |\rightarrow\rangle + |\leftarrow\rangle \\ |\downarrow\rangle_{(x)} & \sim & |\rightarrow\rangle - |\leftarrow\rangle \\ \text{spin along } x & & \text{helicity states} \end{array}$$

- Observables which are sensitive to helicity flip thus give access to transversity PDFs. Poorly known.

- Transversity GPDs are completely unknown experimentally.
- For massless (anti)particles, chirality = (-)helicity
- Transversity GPDs can thus be accessed through chiral-odd Γ matrices.
- Since (in the massless limit) QCD and QED are chiral-even (γ^μ, $\gamma^\mu\gamma^5$), the chiral-odd quantities (1, γ^5, $[\gamma^\mu, \gamma^\nu]$) which one wants to measure should appear in pairs.

Why consider a gamma-meson pair?

Can we probe transversity GPDs in DVMP?

- the leading DA (twist 2) of ρ_T is chiral-odd ($\sigma^{\mu\nu}$ coupling)
- unfortunately $\gamma^* N \to \rho_T N' = 0$, since such a process would require a helicity transfer of 2 from a photon. [Diehl, Gousset, Pire], [Collins, Diehl]
- lowest order diagrammatic argument:

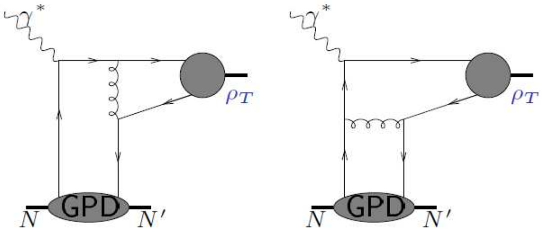

$$\gamma^\alpha[\gamma^\mu, \gamma^\nu]\gamma_\alpha = 0$$

Why consider a gamma-meson pair?
Go to higher twist?

- This vanishing only occurs at twist 2
- At twist 3 this process does not vanish [Ahmad, Goldstein, Liuti], [Goloskokov, Kroll]
- However processes involving twist 3 DAs may face problems with factorisation (end-point singularities)

  can be made safe in the high-energy k_T-factorisation approach

  [Anikin, Ivanov, Pire, Szymanowski, Wallon]

Why consider a gamma-meson pair?
A convenient alternative solution

Circumvent this using 3-body final states:

- $\gamma N \to MMN'$:
  El Beiyad et al. [1001.4491], Enberg et al. [hep-ph/0601138], Ivanov et al. [hep-ph/0209300]
- $\gamma N \to \gamma MN'$:
  Boussarie et al. [1609.03830], Duplancic et al. [1809.08104, 2212.00655, 2302.12026]

Also many others that are not sensitive to chiral-odd GPDs:

- $\gamma N \to \gamma\gamma N'$:
  Pedrak et al. [1708.01043], Grocholski et al. [2110.00048, 2204.00396]
- $\pi N \to \gamma\gamma N'$:
  Qiu, Yu [2205.07846]

- Consider the process $\gamma N \to \gamma M N'$, M =meson. Collinear factorisation of the amplitude at large $M^2_{\gamma M}$, t', and small t.

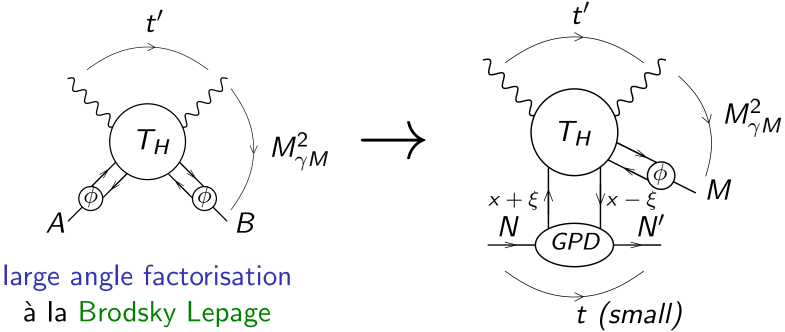

Mesons considered in the final state: $\pi^{\pm}$, $\rho^{\pm,0}_{L,T}$.

How does it work?

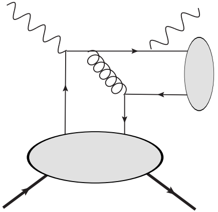

Typical non-zero diagram for a transverse ρ meson

the σ matrices (from either the DA or the GPD) do not kill it anymore!

Why consider a gamma-meson pair?
Is QCD factorisaton really justified?

- Recently, factorisation has been proved for the process $\pi^{\pm} N \to \gamma\gamma N'$ by Qiu, Yu [2205.07846].
- This was extended to a wide range of $2 \to 3$ exclusive processes by Qiu, Yu [2210.07995]
- The proof relies on having large p_T, rather than large invariant mass (e.g. photon-meson pair).
- In fact, NLO computation has been performed for $\gamma N \to \gamma\gamma N'$ by Grocholski et al. [2110.00048].
- Also, NLO computation for $\gamma\gamma \to \pi^+\pi^-$ by crossing symmetry (but involves DAs only) by Duplancic and Nizic [hep-ph/0607069].

$$\gamma(q) + N(p_1) \to \gamma(k) + \rho(p_\rho, \varepsilon_\rho) + N'(p_2)$$

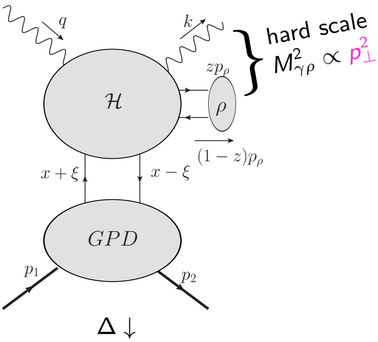

Useful Mandelstam variables:

$$t = (p_2 - p_1)^2$$

$$u' = (p_\rho - q)^2$$

$$t' = (k - q)^2$$

- Factorisation requires:
  $-u' > 1\ \mathrm{GeV}^2$, $-t' > 1\ \mathrm{GeV}^2$ and $(-t)_{\mathrm{min}} \leqslant -t \leqslant .5\ \mathrm{GeV}^2$
  $\Longrightarrow$ sufficient to ensure large p_T.
- Cross-section differential in $(-u')$ and $M^2_{\gamma\rho}$, and evaluated at $(-t) = (-t)_{\mathrm{min}}$.

$$\mathcal{A} = \int_{-1}^{1} dx \int_{0}^{1} dz \; T(x,\xi,z) \; H(x,\xi,t) \; \Phi_\rho(z)$$

- Differential cross section:

$$\left.\frac{d\sigma}{dt\, du'\, dM^2_{\gamma\rho}}\right|_{-t=(-t)_{min}} = \frac{|\overline{\mathcal{A}}|^2}{32 S^2_{\gamma N} M^2_{\gamma\rho} (2\pi)^3} .$$

- Kinematic parameters: $S_{\gamma N}$, $M^2_{\gamma\rho}$ and $-u'$
  Recall: $u' = (p_\rho - q)^2$, $t = (p_2 - p_1)^2$

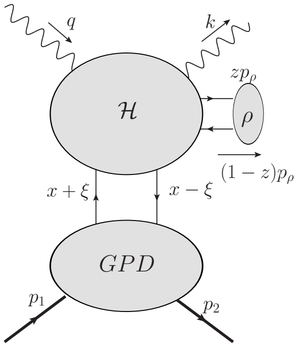

A total of 20 diagrams to compute

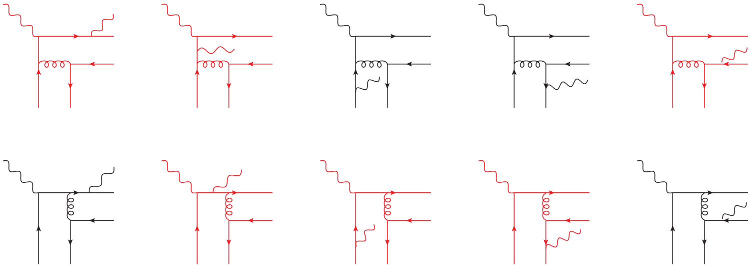

- Need to compute 10 diagrams: Other half related by $q \leftrightarrow \bar{q}$ (anti)symmetry.
- In fact, by choosing the right gauge, only 4 diagrams can be used to generate all the others by various symmetries (eg. photon exchange).
- Red diagrams cancel in the chiral-odd case

For polarised PDFs (and hence transversity PDFs), two scenarios are proposed for the parameterization:

- "standard" scenario, with flavor-symmetric light sea quark and antiquark distributions.
- "valence" scenario with a completely flavor-asymmetric light sea quark densities.

- We take the simplistic asymptotic form of the DAs

$$\phi_{\mathrm{as}}(z) = 6z(1-z)\,.$$

- We also investigate the effect of using a holographic DA:

$$\phi_{\mathrm{hol}}(z) = \frac{8}{\pi}\sqrt{z(1-z)}\,.$$

Suggested by AdS/QCD correspondence [Brodsky, de Teramond], dynamical chiral symmetry breaking on the light-front [Shi et al.], and recent lattice results. [Gao et al.]

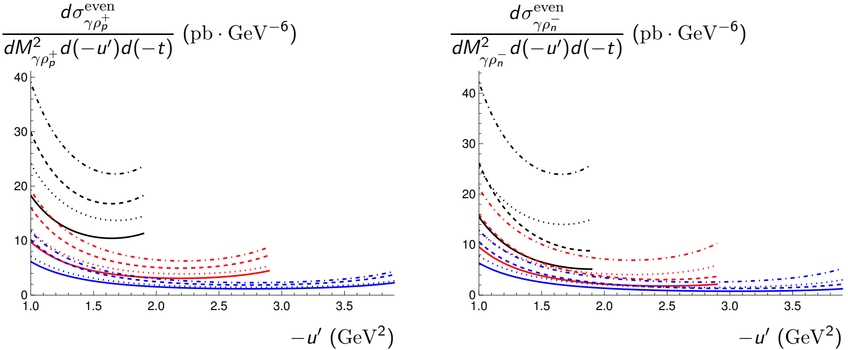

$$S_{\gamma N} = 20\ \text{GeV}^2,\ -t = (-t)_{\text{min}},\ M^2_{\gamma\rho} = 3, 4, 5\ \text{GeV}^2$$

Dashed: Holographic DA non-dashed: Asymptotical DA

Dotted: standard scenario non-dotted: valence scenario

Results

Single differential cross-section: $\rho^+_{p\,L}$ vs π^+_p

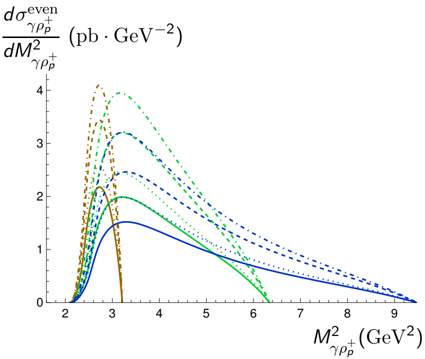

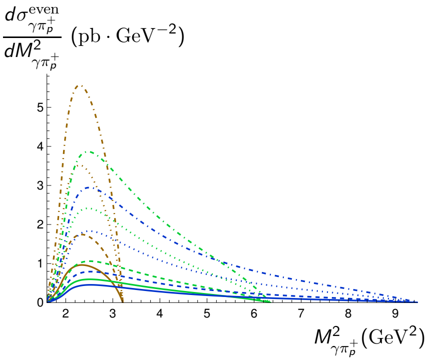

$S_{\gamma N} = 8, 14, 20$ GeV^2

Dashed: Holographic DA non-dashed: Asymptotical DA

Dotted: standard scenario non-dotted: valence scenario

$\Longrightarrow$ Effect of GPD model more important on π^+_p than on ρ^+_p

Results

Single differential cross-section: $\rho_{p\,L}^{+}$ vs $\rho_{p\,T}^{+}$

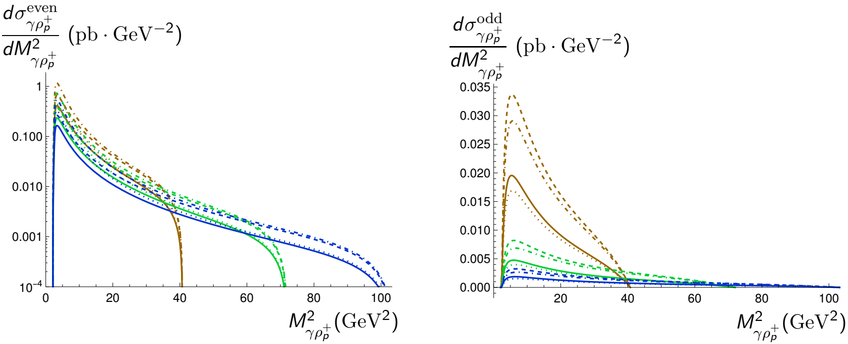

$S_{\gamma N} = 80, 140, 200\ \mathrm{GeV}^2$

Dashed: Holographic DA non-dashed: Asymptotical DA

Dotted: standard scenario non-dotted: valence scenario

$\Longrightarrow$ CO cross-section is suppressed by a factor of ξ^2 ($\xi \approx \frac{M^2_{\gamma\rho}}{2S_{\gamma N}}$).

Integrated cross-section: π_p^+ vs π_n^-

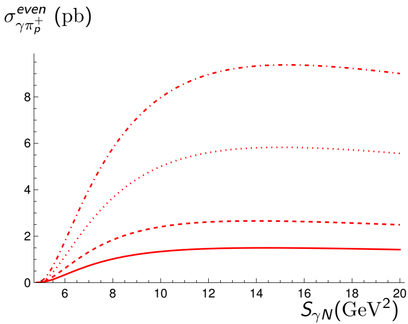

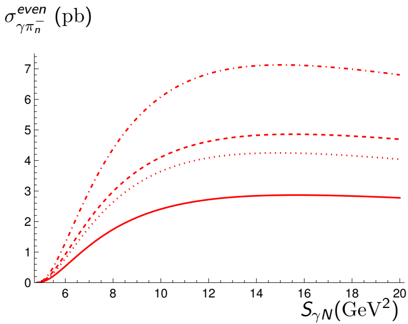

Dashed: Holographic DA   non-dashed: Asymptotical DA

Dotted: standard scenario   non-dotted: valence scenario

$\Longrightarrow$ Huge effect from GPD model in π_p^+ case.

Integrated cross-section: ${\rho_p^+}_L$ vs ${\rho_p^+}_T$

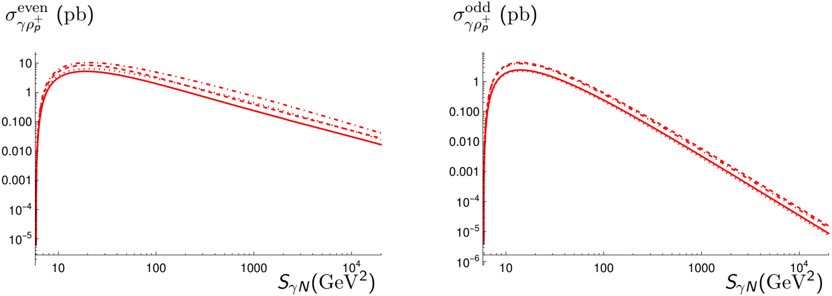

Dashed: Holographic DA non-dashed: Asymptotical DA

Dotted: standard scenario non-dotted: valence scenario

$\Longrightarrow$ ξ^2 suppression in the chiral-odd case causes the cross-section to drop rapidly with $S_{\gamma N}$.

We consider an unpolarised target, and determine polarisation asymmetries wrt the incoming photon.

- Circular polarisation asymmetry $= 0$.
- Linear polarisation asymmetry, LPA $= \frac{d\sigma_x - d\sigma_y}{d\sigma_x + d\sigma_y}$, where x is the direction defined by $p_\perp$ (direction of outgoing photon in the transverse plane).
- In fact,

$$\mathrm{LPA_{Lab}} = \mathrm{LPA}\cos(2\theta)\ ,$$

where θ is the angle between the lab frame x-direction and $p_\perp$.
- Kleiss-Sterling spinor techniques used to obtain expressions.
- Both asymmetries zero in chiral-odd case!

LPA wrt incoming photon: Fully-differential level: $\rho^0_{p\,L}$ vs $\rho^+_{p\,L}$

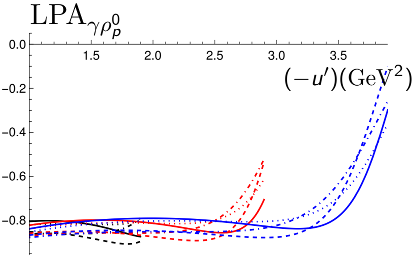

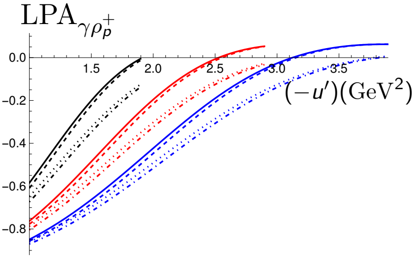

$$S_{\gamma N} = 20\ \mathrm{GeV}^2,\ -t = (-t)_{\min},\ M^2_{\gamma\rho} = 3, 4, 5\ \mathrm{GeV}^2$$

Dashed: Holographic DA non-dashed: Asymptotical DA

Dotted: standard scenario non-dotted: valence scenario

LPA wrt incoming photon: Single-differential level: ${\rho_p^+}_L$ vs π_p^+

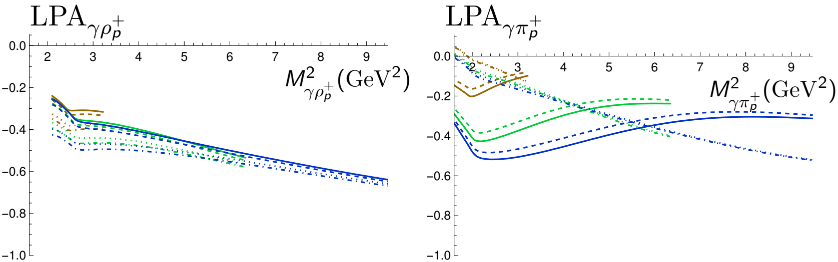

$$S_{\gamma N} = 8,\ 14,\ 20\ \mathrm{GeV}^2$$

Dashed: Holographic DA non-dashed: Asymptotical DA

Dotted: standard scenario non-dotted: valence scenario

$\Longrightarrow$ GPD model changes the behaviour of the LPA completely in the π_p^+ case!

Results

LPA wrt incoming photon: Integrated level: $\rho^-_{n\,L}$ vs π^-_n

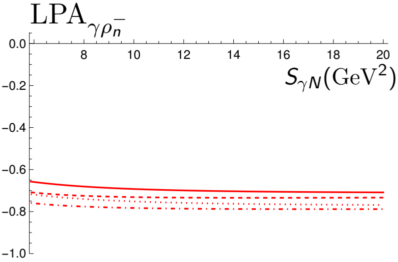

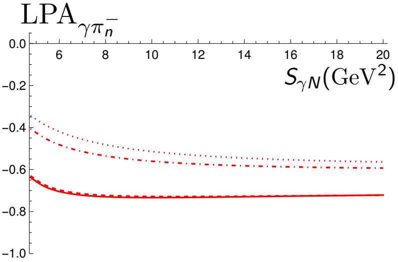

Dashed: Holographic DA non-dashed: Asymptotical DA

Dotted: standard scenario non-dotted: valence scenario

Good statistics: For example, at JLab Hall B:

- untagged incoming $\gamma \Rightarrow$ Weizsäcker-Williams distribution
- with an expected luminosity of $\mathcal{L} = 100\ \mathrm{nb}^{-1}s^{-1}$, for 100 days of run:
  - ρ_L^0 (on p) : $\approx 2.4 \times 10^5$
  - ρ_T^0 (on p) : $\approx 4.2 \times 10^4$ (Chiral-odd)
  - ρ_L^+ : $\approx 1.4 \times 10^5$
  - ρ_T^+ : $\approx 6.7 \times 10^4$ (Chiral-odd)
  - π^+ : $\approx 1.8 \times 10^5$
- No problem in detecting outgoing photon at JLab.

At COMPASS:

- Taking a luminosity of $\mathcal{L} = 0.1 \ \mathrm{nb}^{-1} s^{-1}$, and 300 days of run,
  - ρ_L^0 (on p) : $\approx 1.2 \times 10^3$
  - ρ_T^0 (on p) : $\approx 1.5 \times 10^2$ (Chiral-odd)
  - ρ_L^+ : $\approx 7.4 \times 10^2$
  - ρ_T^+ : $\approx 2.6 \times 10^2$ (Chiral-odd)
  - π^+ : $\approx 7.4 \times 10^2$
- Lower numbers due to low luminosity (factor of 10^3 less than JLab!)

- At the future EIC, with an expected integrated luminosity of $10\,\mathrm{fb}^{-1}$ (about 100 times smaller than JLab):
  - ρ^0_L (on p) : $\approx 2.4 \times 10^4$
  - ρ^0_T (on p) : $\approx 2.4 \times 10^3$ (Chiral-odd)
  - ρ^+_L : $\approx 1.5 \times 10^4$
  - ρ^+_T : $\approx 4.2 \times 10^3$ (Chiral-odd)
  - π^+ : $\approx 1.3 \times 10^4$
- Small ξ study:
  $300 < S_{\gamma N}/\,\mathrm{GeV}^2 < 20000$ ($5 \cdot 10^{-5} < \xi < 5 \cdot 10^{-3}$):
  - ρ^0_L (on p) : $\approx 1.2 \times 10^3$
  - ρ^0_T (on p) : ≈ 6.5 (Chiral-odd) (tiny)
  - ρ^+_L : $\approx 9.3 \times 10^2$
  - π^+ : $\approx 5.0 \times 10^2$

For p-Pb UPCs at LHC (integrated luminosity of 1200 nb^{-1}):

- With future data from runs 3 and 4,
  - $\rho_L^0 : \approx 1.6 \times 10^4$
  - $\rho_T^0 : \approx 1.7 \times 10^3$ (Chiral-odd)
  - $\rho_L^+ : \approx 1.1 \times 10^4$
  - $\rho_T^+ : \approx 2.9 \times 10^3$ (Chiral-odd)
  - $\pi^+ : \approx 9.3 \times 10^3$
- $300 < S_{\gamma N}/\,\text{GeV}^2 < 20000$ ($5 \cdot 10^{-5} < \xi < 5 \cdot 10^{-3}$):
  - $\rho_L^0 : \approx 8.1 \times 10^2$
  - $\rho_L^+ : \approx 6.4 \times 10^2$
  - $\pi^+ : \approx 3.4 \times 10^2$

Conclusion

- Exclusive photoproduction of photon-meson pair provides additional channel for extracting GPDs.
- Especially interesting since it can probe chiral-odd GPDs at the leading twist.
- Proof of factorisation for this family of processes now available.
- Good statistics in various experiments, particularly at JLab.
- Small ξ limit of GPDs can be investigated by exploiting high energies available in collider mode such as EIC and UPCs at LHC.

Outlook

- The processes $\gamma N \to \gamma \pi^0 N'$ and $\gamma N \to \gamma \eta^0 N'$ are of particular interest, since they give access to gluonic GPDs at Born level [ongoing]
- Compute NLO corrections [ongoing]
- Generalise to electroproduction ($Q^2 \neq 0$).
- Add Bethe-Heitler component (photon emitted from incoming lepton)
  - zero in chiral-odd case.
  - suppressed in chiral-even case.

The END

BACKUP SLIDES

Computation

Parametrising the GPDs: ρ_L and π case, Chiral-even

$$\int \frac{dz^-}{4\pi} e^{ixP^+z^-} \langle p_2, \lambda_2 | \bar{\psi}_q \left(-\frac{1}{2}z^-\right) \gamma^+ \psi \left(\frac{1}{2}z^-\right) | p_1, \lambda_1 \rangle$$

$$= \frac{1}{2P^+} \bar{u}(p_2, \lambda_2) \left[H^q(x, \xi, t)\gamma^+ + E^q(x, \xi, t) \frac{i\sigma^{\alpha +}\Delta_\alpha}{2m} \right] u(p_1, \lambda_1)$$

$$\int \frac{dz^-}{4\pi} e^{ixP^+z^-} \langle p_2, \lambda_2 | \bar{\psi}_q \left(-\frac{1}{2}z^-\right) \gamma^+\gamma^5 \psi \left(\frac{1}{2}z^-\right) | p_1, \lambda_1 \rangle$$

$$= \frac{1}{2P^+} \bar{u}(p_2, \lambda_2) \left[\tilde{H}^q(x, \xi, t)\gamma^+\gamma^5 + \tilde{E}^q(x, \xi, t) \frac{\gamma^5\Delta^+}{2m} \right] u(p_1, \lambda_1)$$

- Take the limit $\Delta_\perp = 0$.
- In that case and for small ξ, the dominant contributions come from H^q and $\tilde{H}^q$.

$$\int \frac{dz^-}{4\pi} e^{ixP^+z^-} \langle p_2, \lambda_2 | \bar{\psi}_q \left(-\frac{1}{2}z^-\right) i\sigma^{+i} \psi \left(\frac{1}{2}z^-\right) | p_1, \lambda_1 \rangle$$

$$= \frac{1}{2P^+} \bar{u}(p_2, \lambda_2) \left[H_T^q(x,\xi,t) i\sigma^{+i} + \tilde{H}_T^q(x,\xi,t) \frac{P^+\Delta^i - \Delta^+ P^i}{M_N^2} \right.$$

$$\left. + \quad E_T^q(x,\xi,t) \frac{\gamma^+\Delta^i - \Delta^+\gamma^i}{2M_N} + \tilde{E}_T^q(x,\xi,t) \frac{\gamma^+ P^i - P^+\gamma^i}{M_N} \right] u(p_1, \lambda_1)$$

- Take the limit $\Delta_\perp = 0$.
- In that case and for small ξ, the dominant contributions come from H_T^q.

- GPDs can be represented in terms of Double Distributions [Radyushkin]

$$H^q(x,\xi,t=0) = \int_{-1}^{1} d\beta \int_{-1+|\beta|}^{1-|\beta|} d\alpha\ \delta(\beta+\xi\alpha-x)\, f^q(\beta,\alpha)$$

- ansatz for these Double Distributions [Radyushkin]:
  - chiral-even sector:

$$f^q(\beta,\alpha,t=0) = \Pi(\beta,\alpha)\, q(\beta)\Theta(\beta) - \Pi(-\beta,\alpha)\, \bar{q}(-\beta)\, \Theta(-\beta)\,,$$
$$\tilde{f}^q(\beta,\alpha,t=0) = \Pi(\beta,\alpha)\, \Delta q(\beta)\Theta(\beta) + \Pi(-\beta,\alpha)\, \Delta\bar{q}(-\beta)\, \Theta(-\beta)\,.$$

  - chiral-odd sector:

$$f^q_T(\beta,\alpha,t=0) = \Pi(\beta,\alpha)\, \delta q(\beta)\Theta(\beta) - \Pi(-\beta,\alpha)\, \delta\bar{q}(-\beta)\, \Theta(-\beta)\,.$$

  - $\Pi(\beta,\alpha) = \frac{3}{4}\frac{(1-\beta)^2-\alpha^2}{(1-\beta)^3}$: profile function

- simplistic factorised ansatz for the t-dependence:

$$H^q(x,\xi,t) = H^q(x,\xi,t=t_{\min}) \times F_H(t)$$

with $F_H(t) = \frac{(t_{\min}-C)^2}{(t-C)^2}$ a standard dipole form factor ($C = 0.71\mathrm{GeV}^2$)

Sets of PDFs used to model GPDs

- $q(x)$: unpolarised PDF [GRV-98]

  and [MSTW2008lo, MSTW2008nnlo, ABM11nnlo, CT10nnlo]

- $\Delta q(x)$ polarised PDF [GRSV-2000]

- $\delta q(x)$: transversity PDF [Anselmino *et al.*]

Effects are not significant! But relevant for NLO corrections!

- Helicity conserving (vector) DA at twist 2: ρ_L

$$\langle 0|\bar{u}(0)\gamma^\mu u(x)|\rho_L^0(p)\rangle = \frac{p^\mu}{\sqrt{2}} f_\rho \int_0^1 du\ e^{-iup\cdot x}\phi_\rho(u)$$

- Helicity flip (tensor) DA at twist 2: ρ_T

$$\langle 0|\bar{u}(0)\sigma^{\mu\nu} u(x)|\rho_T^0(p,s)\rangle = \frac{i}{\sqrt{2}}(\epsilon_\rho^\mu p^\nu - \epsilon_\rho^\nu p^\mu) f_\rho^\perp \int_0^1 du\ e^{-iup\cdot x}\ \phi_\rho(u)$$

- Helicity conserving (axial) DA at twist 2: $\pi^\pm$

$$\langle 0|\bar{u}(0)\gamma^\mu\gamma^5 d(x)|\pi(p)\rangle = ip^\mu f_\pi \int_0^1 du\ e^{-iup\cdot x}\phi_\pi(u)$$

Typical kinematic point (for JLab kinematics):
$\xi = .1 \;\leftrightarrow\; S_{\gamma N} = 20\ \mathrm{GeV}^2$ and $M^2_{\gamma\rho} = 3.5\ \mathrm{GeV}^2$

$$\tilde{H}^{q(-)}(x,\xi,t) = \tilde{H}^{q}(x,\xi,t) - \tilde{H}^{q}(-x,\xi,t) \quad [C=-1]$$

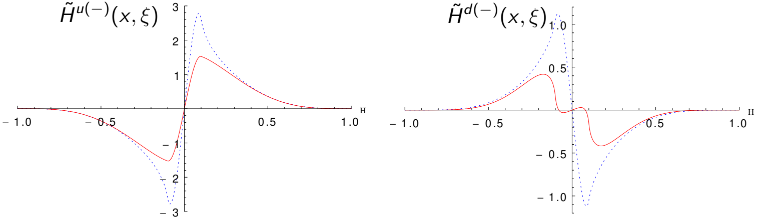

"valence" and "standard": two GRSV Ansätze for $\Delta q(x)$

Computation

Valence vs Standard scenarios in H_T (Chiral-odd)

Typical kinematic point (for JLab kinematics):
$\xi = .1 \;\leftrightarrow\; S_{\gamma N} = 20\ \mathrm{GeV}^2$ and $M^2_{\gamma\rho} = 3.5\ \mathrm{GeV}^2$

$$H_T^{q(-)}(x,\xi,t) = H_T^q(x,\xi,t) + H_T^q(-x,\xi,t) \quad [C=-1]$$

$H_T^{u(-)}(x,\xi)$

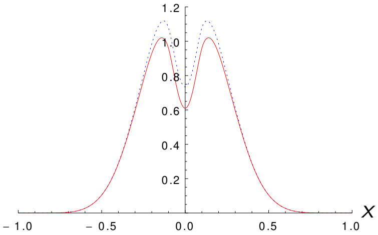

$H_T^{d(-)}(x,\xi)$

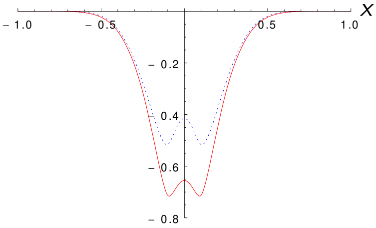

"valence" and "standard": two GRSV Ansätze for $\Delta q(x)$

$\Rightarrow$ two Ansätze for $\delta q(x)$

- Work in the limit of:
  - $\Delta_\perp \ll p_\perp$
  - $M^2,\ m_\rho^2 \ll M_{\gamma\rho}^2$
- initial state particle momenta:

$q^\mu = n^\mu,$
$p_1^\mu = (1+\xi)\, p^\mu + \frac{M^2}{s(1+\xi)} n^\mu$

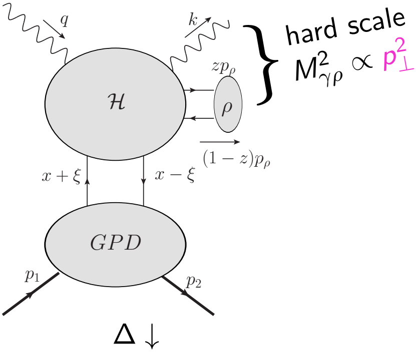

- final state particle momenta:

$$p_2^\mu = (1-\xi)\, p^\mu + \frac{M^2+\vec{p}_t^{\,2}}{s(1-\xi)} n^\mu + \Delta_\perp^\mu$$

$$k^\mu = \alpha\, n^\mu + \frac{(\vec{p}_t - \vec{\Delta}_t/2)^2}{\alpha s} p^\mu + p_\perp^\mu - \frac{\Delta_\perp^\mu}{2}\,,$$

$$p_\rho^\mu = \alpha_\rho\, n^\mu + \frac{(\vec{p}_t + \vec{\Delta}_t/2)^2 + m_\rho^2}{\alpha_\rho s} p^\mu - p_\perp^\mu - \frac{\Delta_\perp^\mu}{2}\,,$$

large angle scattering: $M^2_{\gamma\rho} \sim -u' \sim -t' \quad (S_{\gamma N} = 20 \text{ GeV}^2)$

$\Longrightarrow \; -u' > 1 \text{ GeV}^2$ and $-t' > 1 \text{ GeV}^2$ and $(-t)_{\min} \leqslant -t \leqslant .5 \text{ GeV}^2$

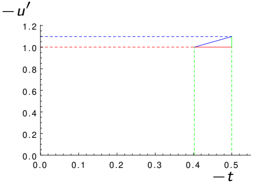

$M_{\gamma\rho} = 2.2 \text{ GeV}^2$

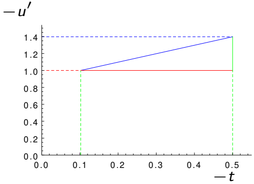

$M^2_{\gamma\rho} = 2.5 \text{ GeV}^2$

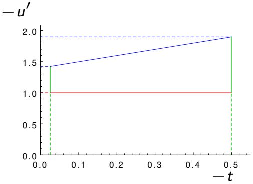

$M_{\gamma\rho} = 3 \text{ GeV}^2$

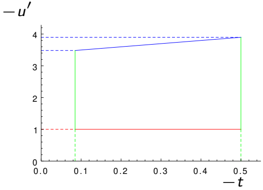

$M_{\gamma\rho} = 5 \text{ GeV}^2$

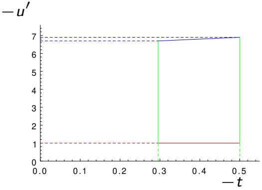

$M_{\gamma\rho} = 8 \text{ GeV}^2$

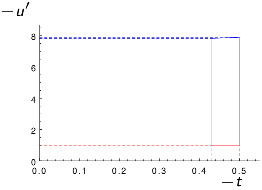

$M_{\gamma\rho} = 9 \text{ GeV}^2$

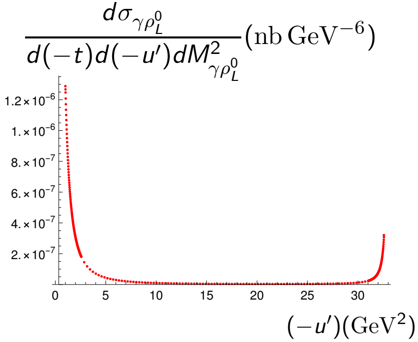

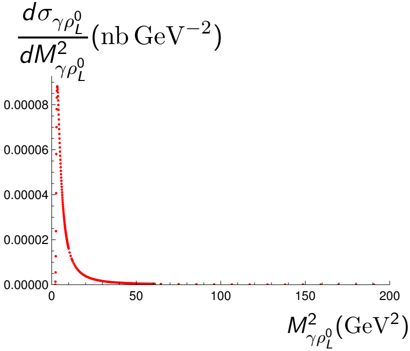

- Need enough points at boundaries for distribution in $(-u')$
- Need enough points to resolve peak (at low $M^2_{\gamma\rho_L^0}$) for distribution in $M^2_{\gamma\rho_L^0}$

Results

Explaining the difference between chiral-even and chiral-odd plots

- $\xi = \frac{M^2_{\gamma M}}{2S_{\gamma N} - M_N^2} \approx \frac{M^2_{\gamma M}}{2S_{\gamma N}}$ for $M^2_{\gamma M} \ll S_{\gamma N}$
- Chiral-even (unpolarised) cross-section:

$$|\overline{\mathcal{M}}_{\mathrm{CE}}|^2 = \frac{2}{s^2}(1-\xi^2)C^2_{\mathrm{CE}}\left\{2\,|N_A|^2 + \frac{p_\perp^4}{s^2}\,|N_B|^2 + \frac{p_\perp^2}{s}\,(N_A N_B^* + c.c.) + \frac{p_\perp^4}{4s^2}\,|N_{A_5}|^2 + \frac{p_\perp^4}{4s^2}\,|N_{B_5}|^2\right\}.$$

- Chiral-odd (unpolarised) cross-section:

$$|\overline{\mathcal{M}}_{CO}|^2 = \frac{2048}{s^2}\xi^2(1-\xi^2)C^2_{\mathrm{CO}}\left\{\alpha^4\,|N_{T\,A}|^2 + |N_{T\,B}|^2\right\}.$$

- Note: $\alpha = \frac{-u'}{M^2_{\gamma M}}$.

To obtain distribution in $S_{\gamma N}$, we exploit non-trivial mapping between 1 set of data at a fixed $S_{\gamma N}$ to other values $\tilde{S}_{\gamma N}$ *lower* than it.

$$\tilde{M}^2_{\gamma M} = M^2_{\gamma M} \frac{\tilde{S}_{\gamma N} - M_N^2}{S_{\gamma N} - M_N^2}\,,$$

$$-\tilde{u}' = \frac{\tilde{M}^2_{\gamma M}}{M^2_{\gamma M}}(-u')\,.$$

Implementing importance sampling $\Longrightarrow$ careful consideration of the various limits involved are needed.

Mapping possible since different sets of $(S_{\gamma N}, M^2_{\gamma M}, -u')$ correspond to the same (α, ξ).

$$\alpha = \frac{-u'}{M^2_{\gamma M}}\,, \qquad \xi = \frac{M^2_{\gamma M}}{2(S_{\gamma N} - M_N^2) - M^2_{\gamma M}}\,.$$

Consider

$$\gamma(q,\lambda_q) + N(p_1,\lambda_1) \to \gamma(k,\lambda_k) + \pi^{\pm}(p_\pi) + N'(p_2,\lambda_2)\ ,$$

where λ_i represent the helicities of the particles.

QED/QCD invariance under parity implies that [Bourrely, Soffer, Leader]

$$\mathcal{A}_{\lambda_2\lambda_k\,;\,\lambda_1\lambda_q} = \eta\,(-1)^{\lambda_1-\lambda_q-(\lambda_2-\lambda_k)}\mathcal{A}_{-\lambda_2-\lambda_k\,;\,-\lambda_1-\lambda_q}\ ,$$

where η represents phase factors related to intrinsic spin.

Thus, at the cross-section level, it is clear that circular asymmetry will vanish, since

$$\sum_{\lambda_i,\,i\neq q}\left|\mathcal{A}_{\lambda_2\lambda_k\,;\,\lambda_1+}\right|^2 = \sum_{\lambda_i,\,i\neq q}\left|\mathcal{A}_{\lambda_2\lambda_k\,;\,\lambda_1-}\right|^2$$

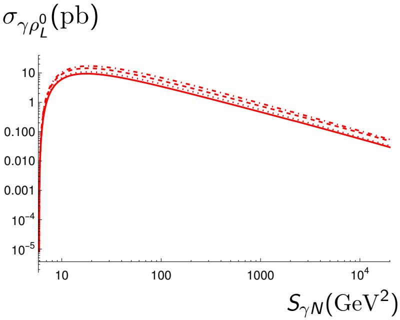

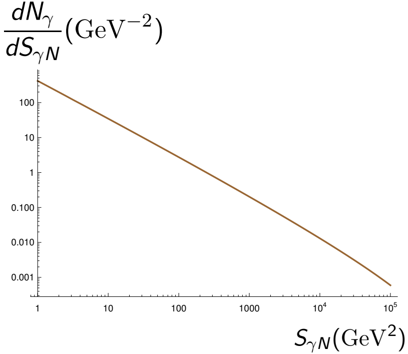

- Photon flux enhanced by a factor of Z^2, but drops rapidly with $S_{\gamma N} \Longrightarrow$ *Low luminosity not compensated by larger photon flux.*
- LHC great for high energy, but JLab better in terms of luminosity.
- Still, LHC gives us access to the small ξ region of GPDs!